

## Synthesis and characterization of one pot electrochemical graphene for supercapacitor applications

R. Naresh Muthu

Department of Physics, J. P. College of Arts and Science, Tenkasi – 627852, Tamilnadu, India  
(Affiliated to Manonmaniam Sundaranar University, Tirunelveli, Tamil Nadu, India)

[rnaresh7708@gmail.com](mailto:rnaresh7708@gmail.com)

**ABSTRACT** Graphene can be used to store energy as well as a supercapacitor material because of its unique physical and chemical properties, including high specific surface area, high chemical stability, high mechanical strength, and oxidation resistance. In this report, a facile, green, and cost-effective approach has been adopted to synthesize graphene sheets through an electrochemical exfoliation technique for supercapacitor applications. Graphene sheets were synthesized using aqueous electrolyte (Ag/AgCl, 0.1 M H<sub>2</sub>SO<sub>4</sub>) with four different exfoliation potentials such as 3, 5, 7 and 9 V. The prepared graphene sheets were subjected to characterization techniques such as Raman spectroscopy, X-ray photoelectron spectroscopy (XPS), X-ray diffraction (XRD), and atomic force microscopy (AFM). The Raman results revealed that the defect density and thickness of the graphene layers increased with increased in the exfoliation potential and then eventually decreased. Among all potentials, the maximum crystalline size of graphene was observed for the potential of 5 V, an intermediate crystalline size of 9 V, and minimum for 7 V, showing that the exfoliated graphene layer was sensitive to the exfoliation potential. XPS study shows the structural oxidation (relative percentage of carbon and oxygen) of the exfoliated graphene at different potentials. The results indicate that electrochemically exfoliated graphene (5 V) has been successfully produced. The behaviour of 5 V graphene has been examined using a charge-discharge (CD) curve and cyclic voltammetry (CV) for supercapacitor applications. The maximum value of specific capacitance obtained is 198 F·g<sup>-1</sup> at a current density of 0.14 A·g<sup>-1</sup> in 6 M KOH. The highest value obtained for energy density and power density is 17 W·h·kg<sup>-1</sup> and 1176 W·kg<sup>-1</sup>.

**KEYWORDS** graphene, electrochemical exfoliation, supercapacitor, EDLC

**FOR CITATION** Naresh Muthu R. Synthesis and characterization of one pot electrochemical graphene for supercapacitor applications. *Nanosystems: Phys. Chem. Math.*, 2023, **14** (3), 380–389.

### 1. Introduction

Due to the continuous depletion of fossil fuels, we require an alternative source of energy. Batteries, fuel cells, and electrochemical supercapacitors are some of the alternative ways to store energy. Supercapacitors got attention because of their distinct features, like high power density, fast charging/discharging rates, high stability, and long-life duration compared to batteries and other electrochemical energy storage devices. Electrochemical supercapacitors can be classified as pseudo-capacitors, electrical double layer capacitors, and hybrid capacitors. Apart from lifetime, energy density and power density are the two parameters for the selection of supercapacitor materials [1, 2].

Graphene is a crystalline allotrope of carbon having a single atomic 2D layer with all carbon having sp<sup>2</sup> hybridization and the remaining electron in the p-orbital form large pi-bond [3]. Due to the presence of a sigma bond, graphene is flexible and stable, the presence of elastic corrugation can bear thermal fluctuation through the modulating bond length. Graphene is attractive due to its exceptional properties [4] including high thermal conductivity ( $\sim 5000 \text{ W}\cdot\text{m}^{-1}\cdot\text{K}^{-1}$ ), high electron mobility ( $15000 \text{ cm}^2\cdot\text{V}^{-1}\cdot\text{s}^{-1}$ ), high current density, high specific surface area ( $2620 \text{ m}^2\cdot\text{g}^{-1}$ ), high mechanical flexibility. The intrinsic capacitance of graphene single layer was found to be  $21 \mu\text{F}\cdot\text{cm}^{-2}$  [5] i.e. the upper limit for electrical double-layer capacitance for carbon-based materials. This suggests that graphene is the ideal carbon electrode material for EDL supercapacitors because the maximum specific capacitance value achieved by graphene when the entire surface of  $2675 \text{ m}^2\cdot\text{g}^{-1}$  is fully utilized is  $550 \text{ F}\cdot\text{g}^{-1}$ .

There are various methods involved in the production of graphene such as Hummer's method, microwave method, chemical vapour deposition (CVD) method, dispersion method and electrochemical exfoliation method. Recently, electrochemical exfoliation of graphene from graphite has attracted researchers due to its easy, cheap and environmental friendly approach to produce high-quality graphene [6].

This report deals with electrochemical exfoliation of graphene from graphite rod in aqueous solution (sulfuric acid) [6–8]. Here SO<sub>4</sub><sup>2-</sup> ions from sulfuric acid (H<sub>2</sub>SO<sub>4</sub>) acts as an exfoliating agent, it gets intercalate between graphite layer and increase the spacing between two consecutive graphite layers, results in graphene layer separation from the

graphite surface. By optimizing the applied potential for electrochemical process, the oxidation of graphene during exfoliation can be reduced. This result suggests that the 5 V exfoliated graphene were relatively higher C/O ratio (from XPS), less defect ratio (from Raman), multiyear graphene (from Raman and AFM) among the 7 and 9 V exfoliated graphene. Based on this, we have chosen 5 V prepared graphene for supercapacitor applications. The specific capacitance of the produced 5 V graphene has been calculated using cyclic voltammetry and charge-discharge curve. It has been found that the maximum specific capacitance value achieved from charging-discharging curve is  $198 \text{ F}\cdot\text{g}^{-1}$ , the maximum energy density and maximum power density calculated are  $17.54 \text{ W}\cdot\text{h}\cdot\text{kg}^{-1}$  and  $1178 \text{ W}\cdot\text{kg}^{-1}$  respectively.

## 2. Experimental section

### 2.1. Materials

Polyvinylidene fluoride (PVDF) membrane (220 nm pore size) and carbon black were supplied by Sigma-Aldrich. Sulfuric acid ( $\text{H}_2\text{SO}_4$ ) 98 %, N-Methyl-2-pyrrolidone (NMP), and potassium hydroxide (KOH) were obtained from Merck. High-purity graphite rods (99.9995 %, 3.05 mm dia, and 305 mm long) and polyvinylidene fluoride (PVDF) were received from Alfa Aesar. All purchased reagents were of analytical grade and used without further purification. Double distilled water was used throughout this study.

### 2.2. Electrochemical exfoliation of graphene

Electrochemical exfoliation of graphite rods (working electrode) were performed using a three-electrode cell configuration with 0.1 M  $\text{H}_2\text{SO}_4$  (0.449 ml of sulfuric acid by using a Sartorius Proline micro pipette to 80 ml of water) as an electrolyte (Ag/AgCl, 0.1 M  $\text{H}_2\text{SO}_4$ ) [9]. The counter electrode was platinum mesh and the reference electrode was an Ag/AgCl. A constant potential of 3, 5, 7 and 9 V was applied for 1 h using Chronoamperometry technique (CHI 660E electrochemical workstation). After exfoliation, the product was collected by vacuum filtration on a polyvinylidene fluoride (PVDF) membrane (220 nm pore size) filter and washed sequentially with deionized water and ethanol until the PH attains 6 – 7 to remove the residual impurities of electrolytes ( $\text{SO}_4^{2-}$ ). Then it was dried at  $100^\circ\text{C}$  for overnight in hot air oven. Finally, electrochemically exfoliated graphene was obtained as fine block powder.

### 2.3. Working electrode preparation for electrochemical supercapacitor applications

**2.3.1. Chemicals and electrode:** The 5 V prepared graphene was used as an active material, polyvinylidene fluoride (PVDF) as a binder, N-methyl-2-pyrrolidone (NMP) as solvent for active material dispersion, carbon black to provide high surface area and cylindrical platinum electrode.

**2.3.2. Working electrode fabrication:** The active material (40 mg), binder PVDF (5 mg) and carbon black (5 mg) are dispersed in 0.5 ml of NMP and mix properly to prepare a thick mixture. This mixture is coated over platinum electrode. Total mass loaded on electrode is 3.4 mg. The electrode then dried in an oven for approximately 24 hours at the temperature of  $60^\circ\text{C}$ . Binder makes the active material attached to the electrode in KOH electrolyte solution. The prepared electrode used for electrochemical characterization.

### 2.4. Characterization

As electrochemically synthesized graphene were subjected to structural, chemical bonding and functional group analysis using characterization techniques. Raman spectroscopy (Thermofischer, 532 nm Ar (green) Laser) was used to characterize the number of graphene layers. The functional groups and oxygen content of the exfoliated samples was determined by X-ray photoelectron spectroscopy (XPS). XPS analysis was performed using an AXIS Supra, Kratos Analytical, with a monochromatic Al K $\alpha$  radiation. High resolution spectra were collected at pass energy is 20 eV. The synthesized graphene sheets were dried at  $120^\circ\text{C}$  for 24 h before the XPS test to minimize the physically absorbed water. The deconvolution of the C 1 s peak was performed by using origin software. X-ray diffraction (XRD) patterns were recorded at room temperature PAN alytical EMPYREAN with Cu K $\alpha$  radiation ( $\lambda = 1.5406 \text{ \AA}$ ) in the range from  $10^\circ$  to  $80^\circ$ . The electrochemical characterization of prepared electrode was performed by an electrochemical workstation (CHI 660 E). A three-electrode system constituting working electrode (graphene coated platinum electrode), counter electrode (platinum mesh) and reference electrode (saturated calomel electrode, SCE) were used to perform cyclic voltammetry and chronopotentiometry analysis. All experiments were performed at ambient temperature and 6 M KOH used as an electrolyte. The cyclic voltammetry (CV) analysis performed at the potential window ranging from  $-1$  to  $0 \text{ V}$  at different scan rate varying from 10 to  $200 \text{ mV}\cdot\text{s}^{-1}$ . The chronopotentiometry charge-discharge analysis is carried out in potential window of  $0.8 \text{ V}$  at different current densities from  $0.3$  to  $3 \text{ A}\cdot\text{g}^{-1}$ . Specific capacitance values  $C_s$  from cyclic voltammetry curves were calculated using equation (1) [11]:

$$C_s = \frac{1}{vm(V_2 - V_1)} \int_{V_1}^{V_2} i(V)dv, \quad (1)$$

where  $C_s$ ,  $V_1$ ,  $V_2$ ,  $i$ ,  $v$ ,  $m$  are specific capacitance ( $\text{F}\cdot\text{g}^{-1}$ ), initial voltage (V), final voltage (V), current (A), scan rate ( $\text{mV}\cdot\text{s}^{-1}$ ) and active mass (g), respectively. The value of integral in numerator was obtained by measuring area under the CVs. The specific capacitance ( $C_{sp}$ ) from charge-discharge curve is calculated using equation (2) [12],

$$C_{sp} = \frac{I\Delta t}{m\Delta V}, \quad (2)$$

where  $I$ ,  $\Delta t$ ,  $m$ ,  $\Delta V$  are current, discharging time, active mass and potential window, respectively.

Energy density ( $E$ ) and Power density ( $P$ ) is calculated by using equations (3) and (4) [11]:

$$E = \frac{1}{2} \left[ \frac{C_{sp} (V_f - V_i)^2}{3.6} \right] \quad (\text{W}\cdot\text{h}\cdot\text{kg}^{-1}), \quad (3)$$

$$P = \frac{3600 \cdot E}{\Delta t} \quad (\text{W}\cdot\text{kg}^{-1}), \quad (4)$$

$V_f$ ,  $V_i$  are final and initial potential respectively.

### 3. Results and discussion

The present work is to optimize the applied potential for getting high-quality graphene via an electrochemical route. During electrochemical exfoliation, the influence of the applied potential (3, 5, 7, and 9 V) was studied, while the rest of the conditions such as solution concentration (0.1 M  $\text{H}_2\text{SO}_4$ ) and reaction time (1 h) were kept constant. There is no exfoliation visible on 3 V.

#### 3.1. Structural and morphological analysis

Raman spectroscopy is a powerful tool for studying the structural quality of synthesized graphene. Fig. 1 depicts the Raman spectra of electrochemically synthesized graphene with 5, 7, and 9 V. For comparison, the Raman spectra of graphite rod is also included in Fig. 1. Raman spectra of graphite and synthesized graphene showed three characteristic peaks located at 1351, 1587, and  $\sim 2698 \text{ cm}^{-1}$  that correspond to the D band, G band, and 2D band, respectively. The G band originates from the vibrations of the  $\text{sp}^2$  hybridized carbon atoms ( $E_{2g}$  mode), whereas the D band arises from lattice distortion (structural defects) in  $\text{sp}^2$  hybridized carbon. The 2D band is attributed to the second order of zone boundary phonons [7, 13]. Graphite shows a less intensity D band, whereas defect is well pronounced in the prepared graphene and indicates the presence of edges and/or topological defects in the basal plane.

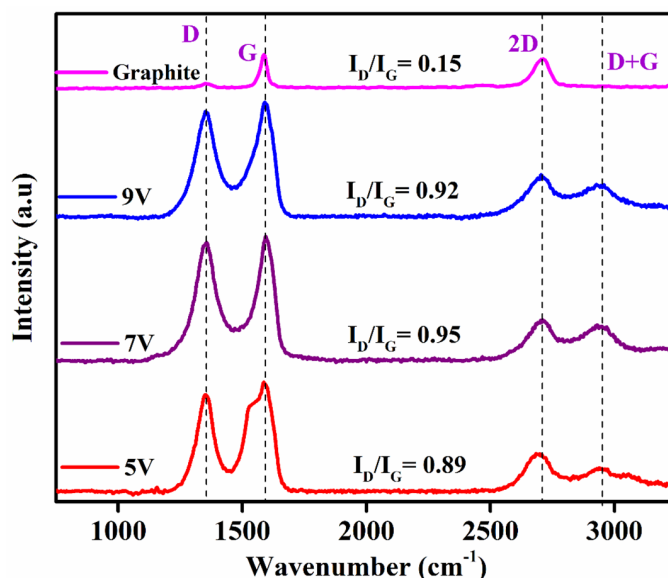


FIG. 1. Raman Spectra of graphite and electrochemically exfol

The intensity ratio of the D and G bands ( $I_D/I_G$ ) gives the amount of defects in synthesized graphene [12]. The 9 V shows an  $I_D/I_G$  value of 0.92, which is larger than 5 V ( $I_D/I_G = 0.8$ ) but smaller than that of 7 V ( $I_D/I_G = 0.95$ ). The increase in  $I_D/I_G$  ratio value indicates the increase in the amount of defects present in the graphene structure when high potential (7 and 9 V) were used, suggesting that a higher defect density is induced by accelerating the oxidation at potential (7 V) as well as the sulphate ions directly forms the  $\text{SO}_2$  gas without interaction at the high anodic potential of 9 V, yield of the exfoliated graphene is very low. The  $I_D/I_G$  ratio value of exfoliated graphene at 5 V was increased to

0.89 from 0.15 of pristine graphite because the  $sp^2$  domains, which are newly formed, are smaller than those of graphite during electrochemical exfoliation.

It is known that the crystallite sizes ( $L_a$ ) are inversely proportional to the  $I_D/I_G$ . The average crystallite size of graphene can be estimated (Table 1) from Tuinstra–Koenig (TK) formula [14].

$$L_a = 2.4 \cdot 10^{-10} \cdot \lambda^4 \cdot (I_D/I_G)^{-1}, \quad (5)$$

where  $\lambda$  is the Raman excitation wavelength. It is found that the crystallite size decreases with increased potential.

TABLE 1. The characteristics of Raman bands of electrochemically exfoliated graphene. The thickness and morphology of the prepared graphene were further examined by AFM

Sample Name	$I_D$ Band	$I_G$ Band	2D Band Peak Position ( $\text{cm}^{-1}$ )	$I_{2D}$ Band	$I_D/I_G$	$I_{2D}/I_G$	Average Crystallite Size (nm)
<b>Graphite</b>	605	4033	2711	162	0.15	0.04	120
<b>5 V</b>	2006	2251	2698	845	0.89	0.38	21.57
<b>7 V</b>	2401	2521	2710	879	0.95	0.35	20.19
<b>9 V</b>	2159	2334	2703	911	0.92	0.39	20.78

The 2D band of 7 and 9 V was located at  $2710 \text{ cm}^{-1}$  (red shift of  $12 \text{ cm}^{-1}$  compared to 5 V) and  $2703 \text{ cm}^{-1}$  (red shift of  $5 \text{ cm}^{-1}$  compared to 5 V), respectively (Fig. 2). The red shift of the 2D band is indicating the increase in the thickness of layer. From Fig. 2, the 2D band of graphite appears at  $2711 \text{ cm}^{-1}$ , exhibiting a red shift from exfoliated graphene at 5 V ( $2698 \text{ cm}^{-1}$ ), and the shape of the 2D band became more symmetrical for graphite in comparison with that of graphene. It suggests that the exfoliated graphene sheets are composed of thinned and multilayered.

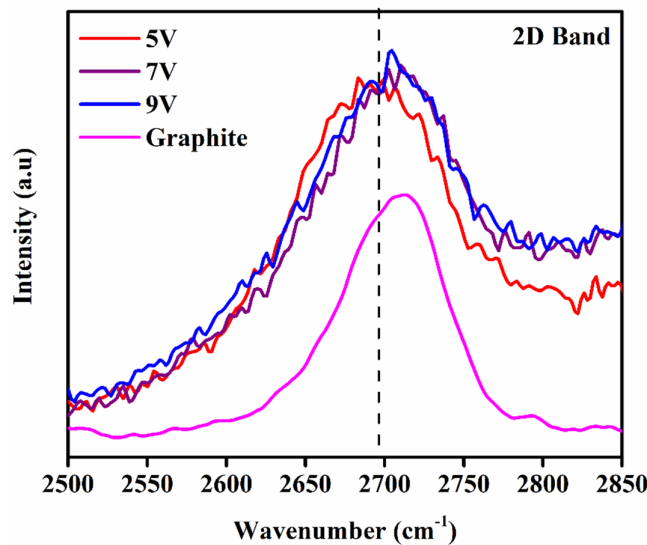


FIG. 2. 2D band spectra of the graphite and electrochemically exfoliated graphene

The intensity ratio of 2D and bands G ( $I_D/I_G$ ) is used to determine the number of graphene layers. The ratio  $I_{2D}/I_G$  is around 2 – 3 for monolayer graphene, 2 – 1 for bi-layer graphene, and  $I_{2D}/I_G \leq 1$  for multilayer graphene [15]. Table 1 summarizes the characteristic Raman G, D, and 2D bands, and their intensity ratio  $I_D/I_G$ ,  $I_{2D}/I_G$  and crystallite size are given for synthesized graphene. The  $I_{2D}/I_G$  graphite is 0.15, and 5 V exfoliated graphene is 0.38. Based on the  $I_{2D}/I_G$  ratio of Raman spectra, it can be suggested that the produced graphene contains multilayers.

X-ray photoelectron spectroscopy (XPS) is used to investigate the nature of the chemical bonding of the graphene. The XPS survey spectra of electrochemically exfoliated graphene are shown in Fig. 3. It clearly shows the presence of C 1s and O 1s peaks at  $\sim 284$  and  $\sim 532$  eV, respectively. The high-resolution scan of C 1s band for 5 V could be fitted with three deconvoluted peaks, whereas 7 and 9 V could be fitted with four deconvoluted peaks (Fig. 4). The deconvoluted peaks at  $284.28 \pm 0.13$ ,  $285.04 \pm 0.28$ ,  $286.41 \pm 0.20$  and  $287.33 \pm 0.24$  eV corresponding to the binding energies of  $sp^2$  Carbon, C–O, C=O and C–O–C, respectively [16, 17]. The major intense peak at  $\sim 284.28$  eV in C 1s spectrum suggests that the presence of  $sp^2$  carbon atoms (C=C) which informs that majority of carbon atoms were arranged in honeycomb structure during electrochemical exfoliation of graphene.

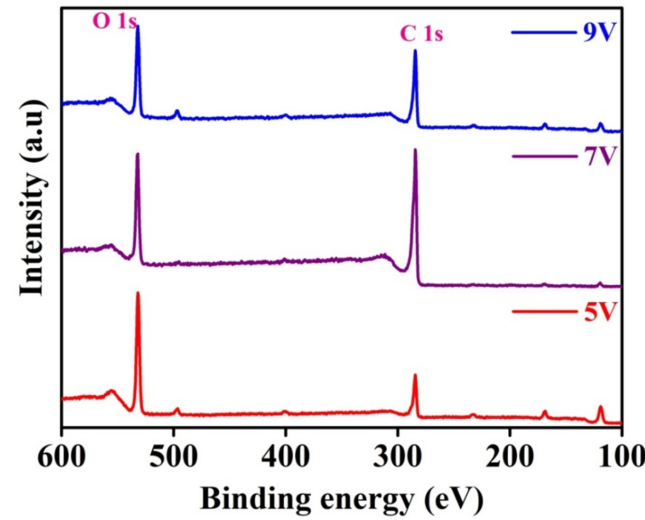


FIG. 3. Full range XPS spectra electrochemically exfoliated graphene

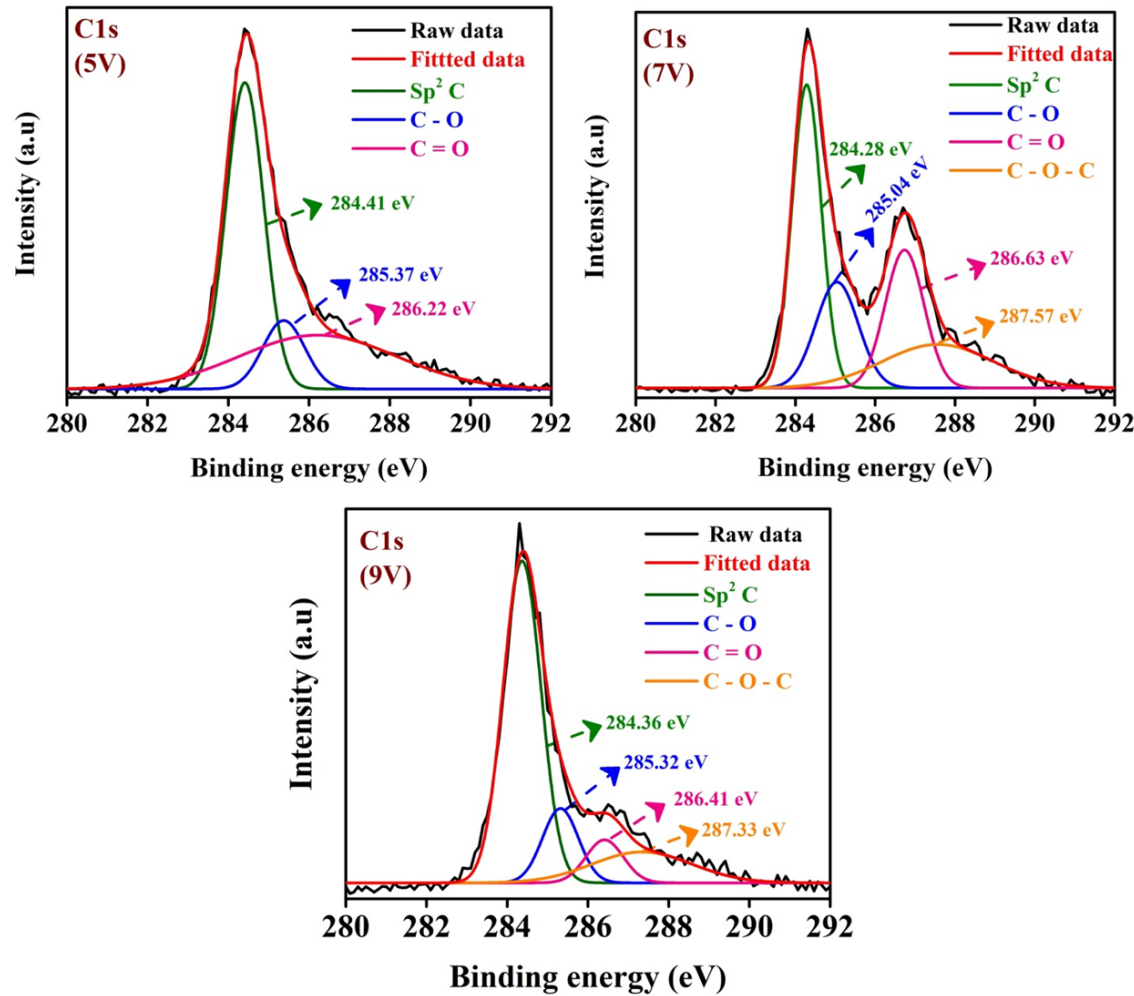


FIG. 4. High resolution XPS spectra of C 1 s for 5, 7, and 9 V

As shown in Table 2, the atomic percentage of carbon and oxygen elements of electrochemical exfoliated graphene. The sample from 5 to 7 V, oxygen element (O at. %) increased from 19 to 48 %. This implies that the oxidation has increased. This is due to increase in  $\text{OH}^-$  and  $\text{SO}_4^{2-}$  ions from 0.1 M  $\text{H}_2\text{SO}_4$ . Interestingly, the amount of O at% in 9 V is (27 %) less than the 7 V but higher than the 5 V. The 5 V exfoliated graphene were relatively higher C/O ratio among the 7 and 9 V exfoliated graphene. This result suggests that during electrochemical exfoliation reaction, small amount of oxygen containing functional groups are formed onto the surface of graphene. It is to be noticed that less amount of oxygen functional groups are present in the electrochemically prepared graphene at 5 V as compared to the other chemical and thermal route, which was previously reported [2, 9, 18].

TABLE 2. Atomic percentages of C and O elements in the synthesized graphene

Sample Name	C 1 s Atomic (%)	O 1 s Atomic (%)	C/O ratio
<b>5 V</b>	81	19	4.23
<b>7 V</b>	52	48	1.09
<b>9 V</b>	73	27	2.66

The Atomic Force Microscopy (AFM) images of graphene prepared at 5, 7 and 9 V are shown in Fig. 5. The AFM images shows that the exfoliated graphene has average thickness of 5.7, 7.6 and 6.5 nm at 5, 7 and 9 V respectively. At the potential of 5 V, minimum thickness observed with 17 graphene layers (multiyear) superimposed on each other. From Fig. 5, it is clearly visible that the graphene sheets appear multilayer, and it is confirmed that some graphitic nanoparticles still need to be exfoliated.

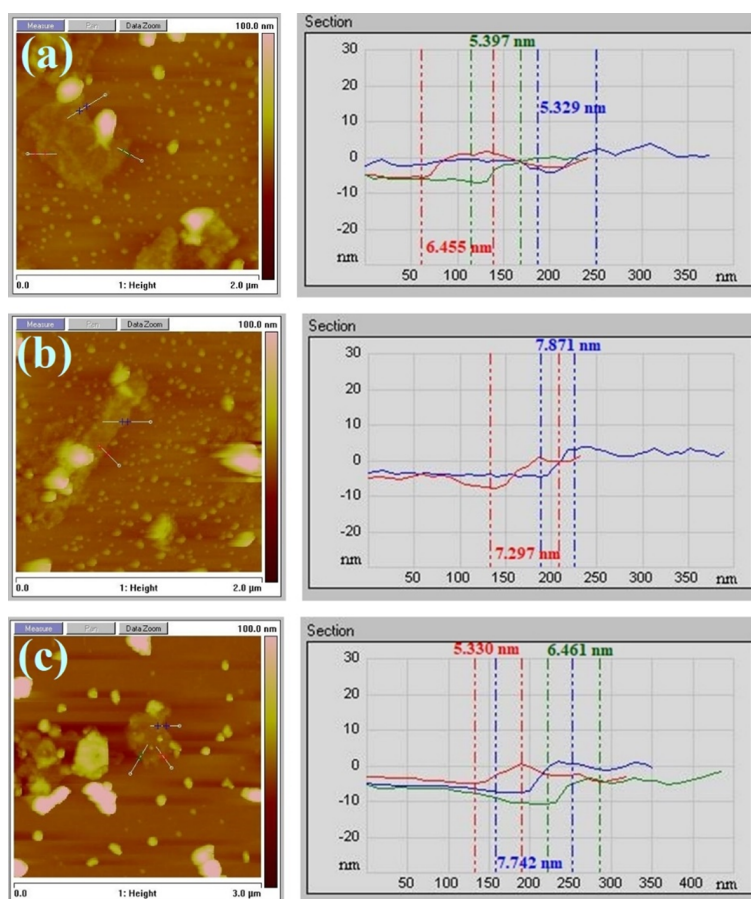


FIG. 5. AFM images (left) and line profile (right) of graphene prepared at 5 V (a), 7 V (b) and 9 V (c)

X-ray diffraction (XRD) analysis was performed to further characterize the synthesized graphene by electrochemical method and purchased graphite rod. Fig. 6 shows the XRD patterns of the graphite rod and synthesized graphene after applying a constant voltage of 5 V. In graphite rod, the peaks that appeared at  $2\theta = 26.6^\circ$ ,  $44.5^\circ$ , and  $54.8^\circ$  correspond to (002), (100), and (004) planes, respectively. The XRD pattern of the synthesized graphene exhibits a much weaker and broader peak center at  $\sim 24.78^\circ$  and  $43.1^\circ$  indexed as (002) and (100) plane, respectively. These two diffraction peaks



indicate the multilayer graphene, which further signifies the efficient exfoliation of graphene and well match with reported literature [2, 9, 18]. Further, the absence of a diffraction peak at  $\sim 11^\circ$  in the prepared sample revealed the absence of graphene oxide, and it was only composed of graphene [18].

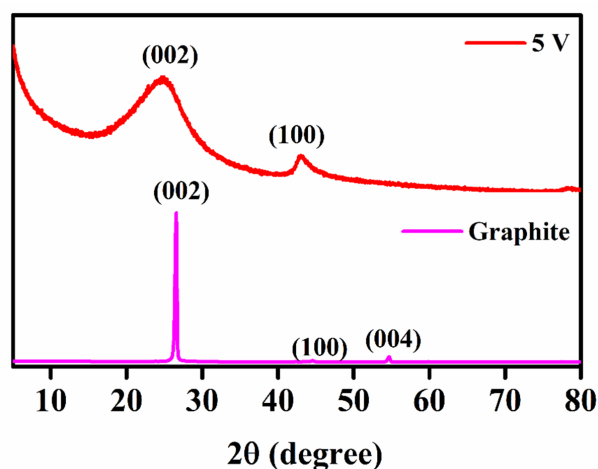


FIG. 6. XRD patterns of graphite rod and graphene prepared at 5 V

The inter-layer spacing at (002) plane of graphite rod and synthesized graphene were calculated by using Bragg's Law:  $2d \sin \theta = n\lambda$ , where  $n = 1$ ,  $\lambda$  is the X-ray wavelength. The estimated inter-layer spacing of the graphite rod was 3.3484 Å, and the synthesized graphene was 3.5901 Å. Compared to graphite, the peak (002) shift with increased inter-layer spacing suggests the poor ordering of sheets along the stacking direction of c-axis. The obtained XRD patterns agree well with the Raman, XPS, and AFM analysis, which confirms the successful preparation of multilayer graphene sheets with low defects.

The present electrochemically exfoliated graphene is definitely feasible to the previously reported chemically prepared graphene. It is noted that our exfoliated graphene produced at 5 V exhibits the less degree of disorder  $I_D/I_G$  from Raman and low oxygen contents (19 %) from XPS and XRD indicates the high structural quality of multilayered graphene with efficiency of 26.3 % (yield) formed. Here, electrochemical exfoliation method, the graphene is attained through a simple intercalation process, so it validates a comparatively lower defect.

### 3.2. Electrochemical performance of 5 V prepared graphene electrode

The electrochemical performance of the synthesised graphene at 5 V was studied through CV and CD. Fig. 7(a) depicts the CV of graphene at a scan rate of  $20 \text{ mV} \cdot \text{s}^{-1}$ . The CVs almost featureless without redox peak and exhibiting rectangular shape indicates an electrical double layer capacitor (EDLC) behaviour between electrode-electrolyte interfaces via non-faradic charging / discharging process. The curves at a different scan rate from 10 to  $200 \text{ mV} \cdot \text{s}^{-1}$  are shown in Fig. 7(b). The value of current density increases with increase in scan rate suggesting fast charging characteristics of electrode. The CVs at all the scan rate of synthesised graphene at 5 V are featureless (there is no peak observed), in the optimized potential range of  $-1.0$  to  $0 \text{ V}$  vs SCE, indicating EDLC [19].

Upon scanning to more negative (cathodic) potentials, diffusion of  $\text{K}^+$  from the electrolyte solution to the electrochemically exfoliated electrode surface was adsorbed through non-faradic reaction. When the scan direction is reversed, and the potential is scanned in the positive (anodic) direction,  $\text{K}^+$  at the graphene electrode surface is depleted.

Figure 8 represent the value of specific capacitance ( $C_s$ ) obtained from CVs, the higher value of specific capacitance observed at slow scan rate and vice-versa. At slow scan rate ions in the electrolyte gets sufficient time to get adsorb over graphene sheets but at high scan rate, charging and discharging process are too fast for the full adsorption and hence lesser surface of electrode used, resulting in low specific capacitance value for higher scan rates and high capacitance value for lower scan rates [19].

Figure 9 (a) depicts the chronopotentiometric charge-discharge (CD) curve of graphene at the current density of  $0.6 \text{ A} \cdot \text{g}^{-1}$ . Fig. 9(b) shows the chronopotentiometric charge-discharge curves at different current densities from  $0.3$  to  $3 \text{ A} \cdot \text{g}^{-1}$  with the voltage ranges from  $-0.1$  to  $-0.8 \text{ V}$  for the same electrode used above for CV. The linear increase in charging curve with constant slope indicates the electrical double layer capacitor behaviour. This result well agrees with the CV studies and consistent with previous report.

Figure 10 shows the values of specific capacitance ranging from  $198$  to  $37 \text{ F} \cdot \text{g}^{-1}$ . Similar to CV, here also increase in current density leads to decrease in specific capacitance. As ion adsorptions over graphene layer reduces with increase in current density.

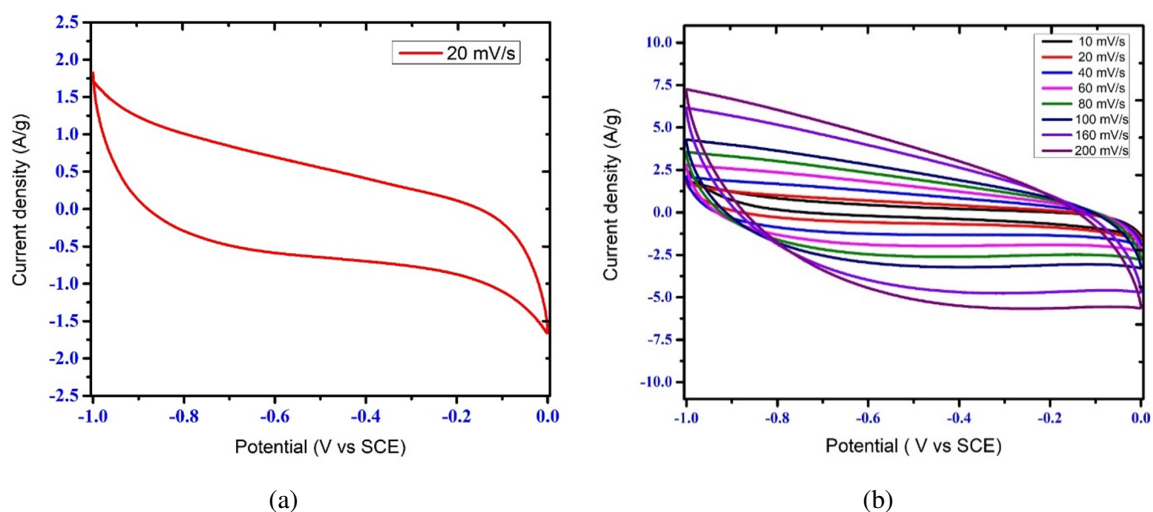


FIG. 7. (a) CV at scan rate of  $20 \text{ mV}\cdot\text{s}^{-1}$ ; (b) CVs at different scan rates

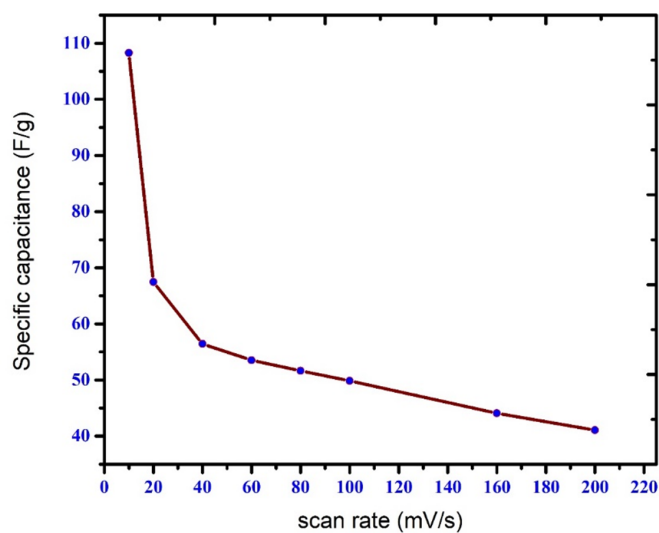


FIG. 8. Specific capacitance at various scan rates ( $10$  to  $200 \text{ mV}\cdot\text{s}^{-1}$ )

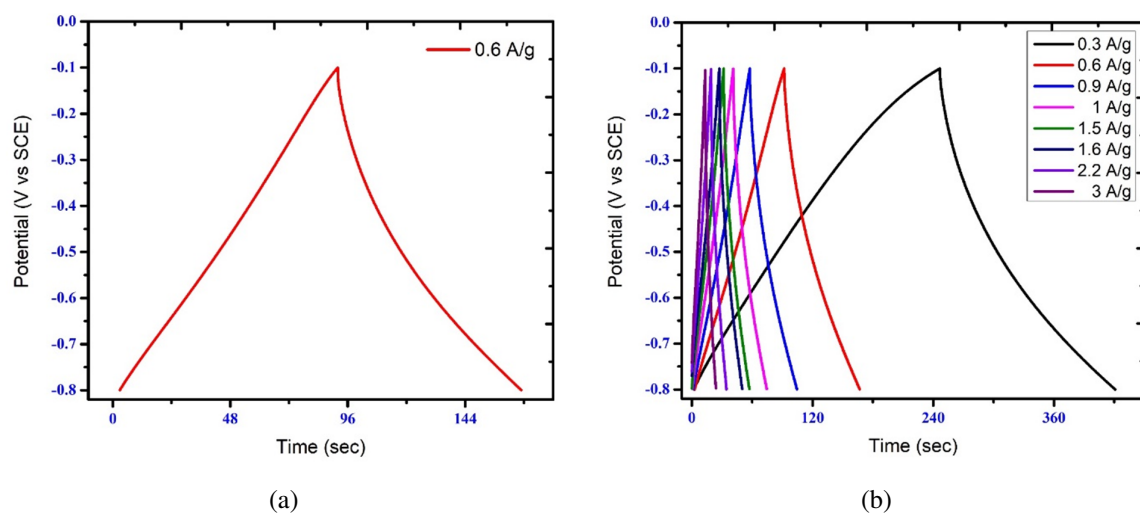


FIG. 9. (a) Charge-discharge curve at current density of  $0.6 \text{ A}\cdot\text{g}^{-1}$ ; (b) Charge-discharge curve at current density varies from  $0.3$  to  $3 \text{ A}\cdot\text{g}^{-1}$



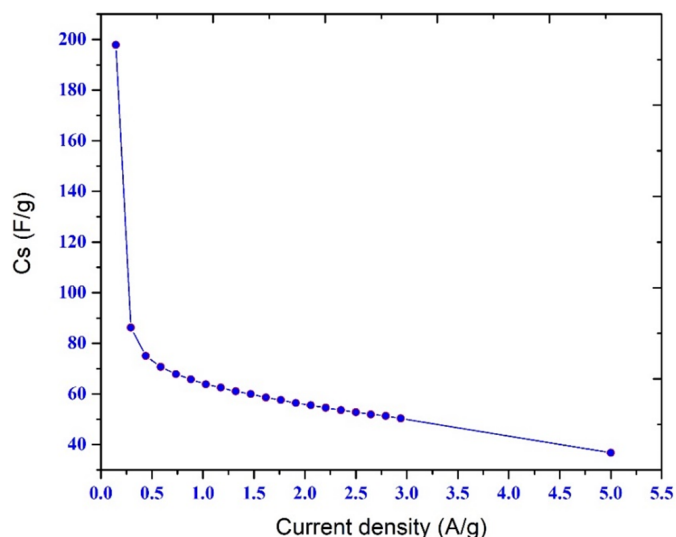
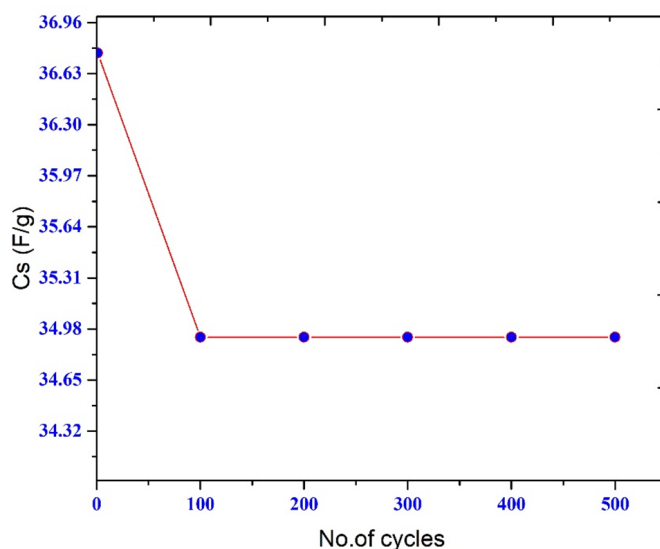


FIG. 10. Specific capacitance at different current density

The cyclic stability of electrode can be observed at a current density of  $5 \text{ A}\cdot\text{g}^{-1}$  from Fig. 11, the value of specific capacitance for 1st and 500th cycle is  $36.76$  and  $34.92 \text{ F}\cdot\text{g}^{-1}$  with the retention of 95 % of the specific capacitance value after 500 cycles, shows that prepared electrode shows excellent stability for supercapacitor behaviour.

FIG. 11. Cyclic stability of graphene electrode at a current density of  $5 \text{ A}\cdot\text{g}^{-1}$ 

Power density and Energy density values calculated from charge-discharge shown in Fig. 12. The maximum power density obtained is  $1176 \text{ W}\cdot\text{kg}^{-1}$  at current density of  $3 \text{ A}\cdot\text{g}^{-1}$ . The maximum energy density obtained is  $17 \text{ W}\cdot\text{h}\cdot\text{kg}^{-1}$ .

#### 4. Conclusion

The present study demonstrates that one-pot synthesis of graphene sheets was fabricated via electrochemical exfoliation with the optimization of applied potential in the presence of  $0.1 \text{ M H}_2\text{SO}_4$  ( $\text{Ag}/\text{AgCl}$ ,  $0.1 \text{ M H}_2\text{SO}_4$ ). The graphene sheets were analysed by XPS, Raman, AFM and XRD. XPS results show the less oxygen content of  $\sim 19.11 \text{ at}\%$  for  $5 \text{ V}$ . AFM exhibits the multi-layer graphene. Raman spectroscopy indicates the low defect density of as-synthesized multi-layer graphene sheets. The XRD result confirms the formation of multi-layer graphene sheets at applied potential of  $5 \text{ V}$ . Hence by using this graphene (prepared at potential of  $5 \text{ V}$ ) to make electrode, by coated on platinum electrode gives specific capacitance of  $198 \text{ F}\cdot\text{g}^{-1}$ , energy density of  $17 \text{ W}\cdot\text{h}\cdot\text{kg}^{-1}$  and power density of  $1176 \text{ W}\cdot\text{kg}^{-1}$  which shows a good EDLC behaviour of electrode in  $6 \text{ M KOH}$  solution.

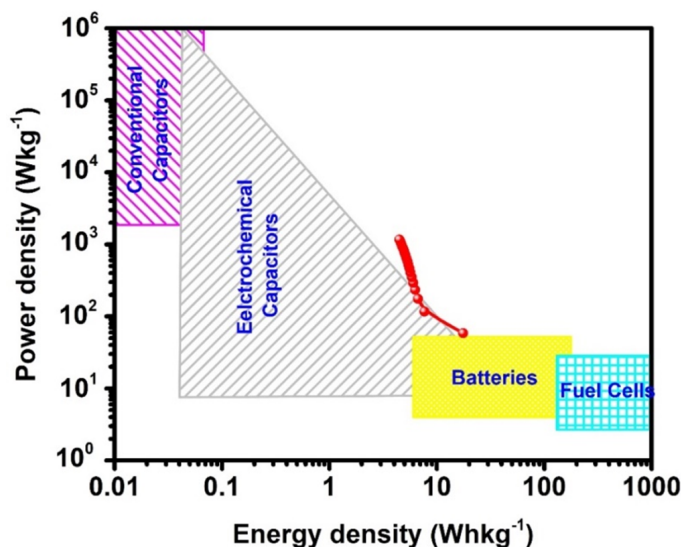


FIG. 12. Ragone plot of prepared graphene electrode compared with different electrochemical devices

## References

- [1] Zhong C., Deng Y., Hu W., Qiao J., Zhang L., Zhang J. A review of electrolyte materials and compositions for electrochemical supercapacitors. *Chem. Soc. Rev.*, 2015, **44** (21), P. 7484–7539.
- [2] Muthu R.N., Tatiparti S.S.V. Electrochemical Behavior of Cobalt Oxide/Boron-Incorporated Reduced Graphene Oxide Nanocomposite Electrode for Supercapacitor Applications. *J. of Mater. Eng. and Perform.*, 2020, **29**, P. 6535–6549.
- [3] Zhong Y., Zhen Z., Zhu H. Graphene: Fundamental research and potential applications. *FlatChem*, 2017, **4**, P. 20–32.
- [4] Rodríguez-Pérez L., Herranz M.Á., Martín N. The chemistry of pristine graphene. *Chem. Commun.*, 2013, **49** (36), P. 3721–3735.
- [5] Liu C., Yu Z., Neff D., Zhamu A., Jang B.Z. Graphene-based supercapacitor with an ultrahigh energy density. *Nano Lett.*, 2010, **10** (12), P. 4863–4868.
- [6] Jibrael R.I., Mohammed M.K.A. Production of graphene powder by electrochemical exfoliation of graphite electrodes immersed in aqueous solution. *Optik (Stuttg.)*, 2016, **127** (16), P. 6384–6389.
- [7] Chen J., Li Y., Huang L., Li C., Shi G. High-yield preparation of graphene oxide from small graphite flakes via an improved Hummers method with a simple purification process. *Carbon N.Y.*, 2015, **81** (1), P. 826–834.
- [8] Pei S., Wei Q., Huang K., Cheng H.M., Ren W. Green synthesis of graphene oxide by seconds timescale water electrolytic oxidation. *Nat. Commun.*, 2018, **9** (1), P. 1–9.
- [9] Muthu R.N., Tatiparti S.S.V. Electrode and symmetric supercapacitor device performance of boron-incorporated reduced graphene oxide synthesized by electrochemical exfoliation. *Energy Storage*, 2020, **2**, e134.
- [10] Arunkumar M., Amit P. Importance of Electrode Preparation Methodologies in Supercapacitor Applications. *ACS Omega*, 2017, **2** (11), P. 8039–8050.
- [11] Pandit B., Dubal D.P., Sankapal B.R. Large scale flexible solid state symmetric supercapacitor through inexpensive solution processed V<sub>2</sub>O<sub>5</sub> complex surface architecture. *Electrochim. Acta*, 2017, **242**, P. 382–389.
- [12] Roldán S., Barreda D., Granda M., Menéndez R., Santamaría R., Blanco C. An approach to classification and capacitance expressions in electrochemical capacitors technology. *Phys. Chem. Chem. Phys.*, 2015, **17** (2), P. 1084–1092.
- [13] Das A.K., et al. Iodide-mediated room temperature reduction of graphene oxide: A rapid chemical route for the synthesis of a bifunctional electrocatalyst. *J. Mater. Chem. A*, 2014, **2** (5), P. 1332–1340.
- [14] Kakaei K., Alidoust E., Ghadimi G. Synthesis of N- doped graphene nanosheets and its composite with urea choline chloride ionic liquid as a novel electrode for supercapacitor. *J. Alloys Compd.*, 2018, **735**, P. 1799–1806.
- [15] Nguyen V.T., Le H.D., Nguyen V.C., Ngo T.T.T., Le D.Q., Nguyen X.N., Phan N.M. Synthesis of multi-layer graphene films on copper tape by atmospheric pressure chemical vapor deposition method. *Adv. Nat. Sci. Nanosci. Nanotechnol.*, 2013, **4** (3), 035012.
- [16] Bindumadhavan K., Chang P-Y., Doong R-a. Silver nanoparticles embedded boron-doped reduced graphene oxide as anode material for high performance lithium ion battery. *Electrochimica Acta*, 2017, **243**, P. 282–290.
- [17] Pullamsetty A., Subbiah M., Sundara R. Platinum on boron doped graphene as cathode electrocatalyst for proton exchange membrane fuel cells. *Int. J. Hydrogen Energy*, 2015, **40** (32), P. 10251–10261.
- [18] Muthu R.N., Rajashabala S., Kannan R. Facile synthesis and characterization of a reduced graphene oxide/halloysite nanotubes/hexagonal boron nitride (RGO/HNT/h-BN) hybrid nanocomposite and its potential application in hydrogen storage. *RSC Adv.*, 2016, **6**, P. 79072.
- [19] Gong Y., Li D., Fu Q., Pan C. Influence of graphene microstructures on electrochemical performance for supercapacitors. *Progress in Natural Science: Materials International*, 2015, **25** (5), P. 379–385.

Submitted 8 February 2023; revised 2 April 2023; accepted 4 April 2023

## Information about the authors:

R. Naresh Muthu – Department of Physics, J. P. College of Arts and Science, Tenkasi – 627852, Tamilnadu, India (affiliated to Manonmaniam Sundaranar University, Tirunelveli); ORCID 0000-0002-4998-7497; rnaresh7708@gmail.com